BIOCHEMISTRY
including biophysical chemistry & molecular biology

Article

pubs.acs.org/biochemistry

Cysteine Is the General Base That Serves in Catalysis by Isocitrate Lyase and in Mechanism-Based Inhibition by 3-Nitropropionate

Margaret M. Moynihan and Andrew S. Murkin*

Department of Chemistry, University at Buffalo, The State University of New York, Buffalo, New York 14260, United States

Supporting Information

ABSTRACT: Isocitrate lyase (ICL) catalyzes the reversible cleavage of isocitrate into succinate and glyoxylate. It is the first committed step in the glyoxylate cycle used by some organisms, including *Mycobacterium tuberculosis*, where it has been shown to be essential for cell survival during chronic infection. The pH−rate and pD−rate profiles measured in the direction of isocitrate synthesis revealed solvent kinetic isotope effects (KIEs) of 1.7 ± 0.4 for ^{D_2O}V and 0.56 ± 0.07 for $^{D_2O}(V/K_{succinate})$. Whereas the ^{D_2O}V is consistent with partially rate-limiting proton transfer during formation of the hydroxyl group of isocitrate, the large inverse $^{D_2O}(V/K_{succinate})$ indicates that substantially different kinetic parameters exist when the enzyme is saturated with succinate. Inhibition by 3-nitropropionate (3-NP), a succinate analogue, was found to proceed through an unusual double slow-onset process featuring formation of a complex with a K_i of 3.3 ± 0.2 μM during the first minute, followed by formation of a final complex with a K_i^* of 44 ± 10 nM over the course of several minutes to hours. Stopped-flow measurements during the first minute revealed an apparent solvent KIE of 0.40 ± 0.03 for association and unity for dissociation. In contrast, itaconate, a succinate analogue lacking an acidic α-proton, did not display slow-binding behavior and yielded a $^{D_2O}K_i$ of 1.0 ± 0.2. These results support a common mechanism for catalysis with succinate and inhibition by 3-NP featuring (1) an unfavorable prebinding isomerization of the active site Cys191−His193 pair to the thiolate−imidazolium form, a process that is favored in D_2O, and (2) the transfer of a proton from succinate or 3-NP to Cys191. These findings also indicate that propionate-3-nitronate, which is the conjugate base of 3-NP and the "true inhibitor" of ICL, does not bind directly and must be generated enzymatically.

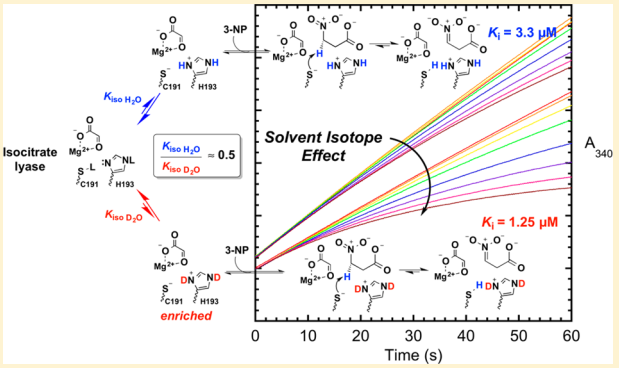

Isocitrate lyase (ICL, EC 4.1.3.1) catalyzes the reversible cleavage of isocitrate into succinate and glyoxylate. It is the first committed step in the glyoxylate cycle used by many organisms like plants, nematodes, fungi, and bacteria such as *Mycobacterium tuberculosis* and has not been identified in humans.[1,2] *M. tuberculosis* isocitrate lyase (*Mt*ICL) has been shown to be essential for cell survival during chronic infection by the mycobacterium, where there is a shift in carbon sources from carbohydrates to fatty acids and acetate, upregulating the glyoxylate cycle and decreasing the level of glycolysis.[1,3] *In vivo* experiments have shown that disruption of the genes encoding *Mt*ICL has weakened the bacterium's ability to grow in mice and has led to rapid elimination from the lungs and spleen.[4] *Mt*ICL's role in virulence for chronic stages of tuberculosis has made it a popular drug target, but mechanistic questions remain.

The synthesis of isocitrate from glyoxylate and succinate, the reverse of the physiological reaction, proceeds through an aldol-type reaction in which deprotonation of the *pro-S* proton at C-2 of succinate is accompanied by formation of a carbon−carbon bond between this carbon and C-2 of glyoxylate (Scheme 1).[5] Previous studies have shown that a solvent-derived proton is incorporated into succinate during isocitrate cleavage.[6] Crystal structures of *Mt*ICL[7] and its orthologues from *Escherichia coli*[8] and *Aspergillus nidulans*[2] have revealed that a conserved cysteine residue (Cys191 in *Mt*ICL) is in the proximity of C-2 of succinate, suggesting that it is responsible for proton transfer. Mutagenesis studies of the *E. coli* enzyme emphasized the importance of this cysteine for catalysis.[9]

Scheme 1

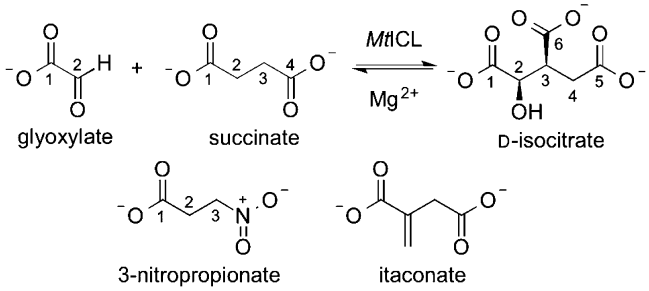

Received: October 21, 2013
Revised: November 22, 2013
Published: December 19, 2013

In this article, we assess the role of Cys191 as a general base for succinate deprotonation by exploiting the sulfhydryl's unique deuterium fractionation factor through the measurement of solvent kinetic isotope effects on isocitrate synthesis. Further, by determining solvent isotope effects on the inhibition constants for itaconate and 3-nitropropionate (3-NP), we demonstrate that the latter acts as a mechanism-based inhibitor and is not bound directly in its nitronate form, as had been previously suggested.[10] Chemical mechanisms are proposed to account for these new data.

EXPERIMENTAL PROCEDURES

Materials. The gene encoding *Mt*ICL was obtained synthetically (DNA 2.0, Menlo Park, CA) inserted into the pJexpress 404 vector by the supplier. The DNA sequence was optimized for *E. coli* codon usage and encodes a thrombin-cleavable N-terminal His_6 tag (MHHHHHHLVPRGSH) fused to the native protein from *M. tuberculosis* strain H37R.[11] Deuterium oxide contained 99.8% D. Stock solutions of glyoxylate, prepared from glyoxylic acid monohydrate by adjusting the pH to 7 with 1 M KOH, were quantified by the method of Dixon and Kornberg by forming the phenylhydrazone (ε_{324} = 17 mM^{-1} cm^{-1}).[12] Concentrations of D-isocitrate in stock solutions of trisodium DL-isocitrate were determined spectrophotometrically by the amount of NADPH (ε_{340} = 6.22 mM^{-1} cm^{-1}) produced using isocitrate dehydrogenase (IDH; see below) and excess $NADP^+$. Concentrations of stock solutions of disodium succinate were determined spectrophotometrically by the amount of NADPH produced using *Mt*ICL, IDH, and excess glyoxylate and $NADP^+$. Concentrations of stock solutions of itaconate and 3-NP were determined gravimetrically from their acid forms, which were neutralized with 1 M KOH.

Isocitrate Lyase Expression and Purification. BL21-(DE3) *E. coli* cells transformed by the supplier (DNA 2.0) with the plasmid encoding *Mt*ICL were grown at 37 °C to an OD_{600} of 0.5−0.6 in LB-Miller broth containing 100 mg/L ampicillin. Optimal protein expression was achieved via induction by isopropyl β-D-1-thiogalactopyranoside (IPTG) to a final concentration of 50 μM and incubation at 31 °C for 4 h. Cells were lysed in 50 mM Tris-HCl (pH 7.5) containing 0.5 M NaCl and a cOmplete protease inhibitor cocktail tablet (Roche Applied Science) through an M-110L pneumatic cell processor (Microfluidics). The lysate was clarified by centrifugation at 15000*g* for 60 min at 4 °C, and the supernatant was loaded onto a Ni^{2+} HisPrep FF 16/10 column using an AKTA fast performance liquid chromatography system (GE). The column was washed with buffer consisting of 50 mM Tris-HCl (pH 7.5), 0.5 M NaCl, and 25 mM imidazole before the protein was eluted using a linear gradient of increasing imidazole concentrations (25 to 500 mM). The column fractions were evaluated using sodium dodecyl sulfate−polyacrylamide gel electrophoresis alongside a molecular mass ladder, and fractions containing the 48 kDa protein were pooled, dialyzed, and stored in 50 mM MOPS (pH 6.8), 100 mM NaCl, and 10% glycerol. The protein concentration was determined by the absorbance at 280 nm using an ε_{280} of 50.8 mM^{-1} cm^{-1} (determined experimentally via a Bradford assay[13]). The expression and purification yielded approximately 20 mg of protein/L of culture.

Coupling Enzyme Expression and Purification. BL21-(DE3) *E. coli* cells previously transformed with a plasmid resulting from the insertion of the gene encoding either *E. coli* isocitrate dehydrogenase (IDH) or *E. coli* lactate dehydrogenase (LDH) into pCA24N were obtained from the National BioResource Project, Japan (NBRP-*E. coli* at NIG).[14] Cultures were inoculated and grown at 37 °C to an OD_{600} of 0.5−0.6 in LB-Miller broth containing 25 μg/L chloramphenicol. Optimal expression was achieved via induction with 500 μM IPTG at 37 °C overnight for IDH and 50 μM IPTG at 31 °C for 4 h for LDH. Cell lysis and protein purification and storage were performed as described for *Mt*ICL, yielding 120 mg/L of culture at 84 units/mg of protein for IDH and 48 mg/L of culture at 63 units/mg of protein for LDH. Units are defined as the amount of enzyme required to reduce 1 μmol of $NADP^+$/min at 37 °C for IDH or to reduce 1 μmol of glyoxylate/min at 37 °C for LDH.

Steady-State Kinetics at a Fixed pH. Unless stated otherwise, all measurements were performed at 37 °C in 50 mM MOPS (pH 7.0) containing 5 mM $MgSO_4$. *Mt*ICL activity was measured spectrophotometrically in the isocitrate cleavage direction by monitoring the oxidation of NADH (0.2 mM) at 340 nm (ε_{340} = 6.22 mM^{-1} cm^{-1}) in a lactate dehydrogenase-coupled assay,[15,16] and in the isocitrate condensation direction by monitoring the reduction of $NADP^+$ (0.2 mM) in an IDH-coupled assay. Substrate (isocitrate, succinate, or glyoxylate) concentrations were varied, and the reactions were initiated by the addition of 30 nM *Mt*ICL (monomers). In either assay, the units of the coupling enzyme present were at least 10-fold greater than the units of *Mt*ICL. Initial velocities were fit by nonlinear regression to eq 1 using KaleidaGraph (Synergy Software) for isocitrate cleavage and globally fit by nonlinear regression to eq 2 using SigmaPlot (Systat) or the Solver add-in in Microsoft Excel[17] for isocitrate synthesis. Equation 2 governs an ordered sequential mechanism with substrate inhibition via a dead-end EA_2 complex,[18] in which [A] and [B] are concentrations of glyoxylate and succinate, respectively, K_a and K_b are the respective Michaelis constants, and K_{ia} and K_i are the dissociation constants for glyoxylate from the EA and EA_2 complexes, respectively.

$$\frac{v_0}{[E]_t} = \frac{k_{cat}[S]}{[S] + K_m} \quad (1)$$

$$\frac{v_0}{[E]_t} = (k_{cat}[A][B])/[K_{ia}K_b + K_a[B] + K_b[A] (1 + [A]/K_i) + [A][B]] \quad (2)$$

pL Profiles with Succinate as the Varied Substrate. Isocitrate synthesis was monitored as described above with a glyoxylate concentration fixed at 500 μM and succinate varied in the following buffers (50 mM): MES (pL 5.0−6.5), MOPS (pL 6.5−7.5), HEPES (pL 7.5−8.5), and CHES (pL 8.5−9.5). Note that DTT was not included for the data presented in Figure 1 and Table 2; however, following discovery that *Mt*ICL is stabilized by DTT over extended incubations (see pH Dependence of Inhibition Constants), for the sake of consistency, k_{cat} and k_{cat}/K_b were redetermined at pL 6.0, 6.5, 7.0, and 7.5 in the presence of 1 mM DTT. Both kinetic parameters were lower than in the absence of DTT but by a constant factor in H_2O and D_2O (~15% lower for k_{cat} and 35% lower for k_{cat}/K_b), indicating that the pL−rate profiles and solvent KIEs would not be significantly altered. To ensure consistency, buffers and solutions of glyoxylate, $MgSO_4$, and $NADP^+$ were prepared and pH values adjusted in H_2O, divided into two portions, rotary evaporated, and reconstituted to the

dx.doi.org/10.1021/bi401432t | *Biochemistry* 2014, 53, 178−187

original volume in the respective solvent (H_2O or D_2O). A 1 M stock solution of succinate prepared in H_2O was serially diluted in either H_2O or D_2O to give 100 and 10 mM solutions, from which up to 100 μL was transferred into each cuvette. Reactions in H_2O or D_2O were initiated by the addition of 10 μL of 1 μM *Mt*ICL (monomers) prepared in buffered H_2O. Thus, the reaction mixtures in D_2O contained 1−2% H_2O, which was considered negligible in light of other sources of error. The same pL was assayed for both solvents on the same day. The pL values of the cuvettes were checked using a Mettler Toledo FE20 probe, and samples in D_2O were corrected according to the equation pD = meter reading + 0.4.[19] The initial velocity was analyzed by nonlinear regression fitting to eq 1 using KaleidaGraph (Synergy Software). Data for pL profiles on the apparent k_{cat}/K_b in H_2O and D_2O were fit to eqs 3 and 4, respectively, and data for the apparent k_{cat} were fit to eq 5[20]

$$(k_{cat}/K_b)_{app} = \frac{c}{1 + 10^{(pK_1 - pH)} + 10^{(pH - pK_2)}[1 + 10^{(pH - pK_3)}]} \quad (3)$$

$$(k_{cat}/K_b)_{app} = c/\left(1 + 10^{pK_1 - pD} + 10^{pD - pK_2}\right) \quad (4)$$

$$(k_{cat})_{app} = \frac{c(1 + \gamma \times 10^{pK_1 - pL})}{1 + 10^{pK_1 - pL} + 10^{pL - pK_2}} \quad (5)$$

where c is the corresponding pL-independent limit, K_1, K_2, and K_3 are the apparent acid dissociation constants, and γ is a partial activity factor that accounts for the non-zero activity of the fully protonated species at low pH.[21] The isotope effects on the apparent k_{cat} and k_{cat}/K_b were determined as c_{H_2O}/c_{D_2O}.

pH Dependence of Inhibition Constants. Isocitrate formation in the presence of varying concentrations (1−5000 μM) of itaconate or 3-NP was measured in cuvettes at different pH values containing 50 mM buffer (see above for buffer choices for each pH range), 5 mM $MgSO_4$, 1 mM DTT, 0.2 mM $NADP^+$, 500 μM glyoxylate, 200 μM succinate, and 0.1 unit of IDH. *Mt*ICL was observed to lose substantial activity in prolonged incubations at 37 °C in the absence of DTT but retained most of its activity in its presence, losing <15% upon being incubated for >300 min at this temperature. Thus, DTT was included in all inhibition experiments. Reactions were initiated with 10 nM *Mt*ICL (monomers). For 3-NP inhibition, the initial velocity was limited to the first 3 min, to minimize slow-onset inhibition effects. The K_i value at each pH was calculated by first determining IC_{50} using eq 6

$$v_i = \frac{v_0 IC_{50}}{[I] + IC_{50}} \quad (6)$$

where v_i and v_0 are the initial velocities in the presence and absence of inhibitor, respectively, and then by applying the Cheng−Prusoff equation (eq 7)

$$K_i = \frac{IC_{50}}{1 + \frac{[B]}{K_b}} \quad (7)$$

where B is succinate and K_b is its Michaelis constant at the given pH. The pK_i values were plotted versus pH, and the data were fit to eq 8 for 3-NP and eq 9 for itaconate, where p$K_{i\,lim}$ is the pH-independent pK_i.[20]

$$pK_i = pK_{i\,lim} - \log(1 + 10^{pK_1 - pH} + 10^{pH - pK_2}) \quad (8)$$

$$pK_i = pK_{i\,lim} - \log[1 + 10^{pH - pK_1}(1 + 10^{pH - pK_2})] \quad (9)$$

Equation 8 describes a double-ionization model in which one group must be protonated and the other deprotonated for binding, while eq 9 describes a model in which two groups must be protonated for binding.

Steady-State Inhibition of *Mt*ICL by 3-Nitropropionate. The inhibition of *Mt*ICL by 3-NP following the slow-onset period was determined following overnight incubation of the inhibitor with the enzyme. Samples (1 mL) containing 50 mM HEPES (pH 7.5), 5 mM $MgSO_4$, 500 μM $NADP^+$, 1 mM DTT, 500 μM glyoxylate, 0.1 unit of IDH, 3 nM *Mt*ICL, and varying concentrations of 3-NP (0.01−5 μM) were incubated for 18 h at 37 °C. From each tube, 950 μL was added to a cuvette and the reaction was initiated by addition of 50 μL of 10 mM succinate (500 μM final). The K_i* was calculated from eqs 6 and 7.

Solvent Isotope Effect on the Itaconate Inhibition Constant. Activity was monitored using the IDH-coupled assay described above in 50 mM HEPES buffer (pL 7.5), with the succinate concentration fixed at 200 μM and the itaconate concentration at 0.05−500 μM. A 1 M stock solution of itaconate prepared in H_2O was serially diluted in either H_2O or D_2O to give 100 and 10 mM solutions, from which up to 100 μL was transferred into each cuvette. Reactions were initiated with 10 μL of 1 μM *Mt*ICL (prepared in buffered H_2O). Thus, the reaction mixtures in D_2O contained 1−2% H_2O. K_i values were obtained by fitting the data to eqs 5 and 6, using K_b values determined from assays in the absence of inhibitor performed on the same day using the same solutions.

Solvent Isotope Effect on 3-NP Inhibition. Activity was monitored using an Applied Photophysics SX20 stopped-flow spectrometer fit with a 20 μL flow cell with a dead time of 1 ms. Transients from four to six repeat drives were averaged for all stopped-flow assays. A 1 cm path length was used, and the reaction chamber and all reagents were thermostated at 37.0 °C with a circulating water bath. Solutions in both syringes, prepared in either H_2O or D_2O, contained 50 mM HEPES (pL 7.5), 5 mM $MgSO_4$, 0.2 mM $NADP^+$, 1 mM DTT, and 500 μM glyoxylate. In addition, one syringe was loaded with 0.2 unit/mL IDH and 400 nM *Mt*ICL and the other with 1 mM succinate and varying concentrations of 3-NP. A 100 mM stock solution of 3-NP was prepared in H_2O and then diluted to 100 μM with either H_2O or D_2O. Because of the slow exchange of deuterium into 3-NP, the D_2O version of this 100 μM solution was freshly prepared from the concentrated stock immediately before each trial and stored on ice for no longer than 70 min. One minute prior to injection, the appropriate volume of this solution was added to the rest of the syringe solution already equilibrated in D_2O at 37 °C; this treatment exposed 3-NP to D_2O at this temperature for a maximum of 12 min. Final concentrations of 3-NP in the observable cell ranged from 1 to 10 μM for D_2O and from 1 to 25 μM for H_2O. Reactions, initiated by 1:1 mixing, were monitored at 340 nm for 60 s, sampling data every 0.06 s.

Transients were fit with eq 10

$$y(t) = Ae^{-k_{obs}t} + c \quad (10)$$

where $y(t)$ is the observed absorbance signal at time t, A is the amplitude of the transient, and c is the absorbance offset. Secondary replots of k_{obs} versus 3-NP concentration were fit with eq 11[22,23]

$$k_{obs} = k_{off} + (k_{on})_{app}[I] \quad (11)$$

where $(k_{on})_{app}$ is the apparent rate constant for association and deprotonation of 3-NP and k_{off} is the net rate constant for protonation of the nitronate and dissociation.

Determination of the Succinate K_m by Stopped-Flow Spectroscopy. Because of the dependence of k_{obs} on the degree of saturation with succinate (eq 11), K_b was determined accurately in H_2O and D_2O using the same conditions described above for the solvent isotope effect measurements with 3-NP, except in the absence of the inhibitor and with final succinate concentrations ranging from 25 to 5000 μM. The transients, monitored for 60 s, were fit to a linear function to obtain the initial velocities, and the K_b was obtained by fitting to eq 1.

RESULTS

Steady-State Kinetics of *Mt*ICL. Steady-state kinetics for *Mt*ICL were determined in both reaction directions at pH 7.0 and 37 °C (Table 1). The K_m of 45 μM for isocitrate agrees with the reported value measured at pH 7.5 and 25 °C.[24] The k_{cat} of 12.2 s^{-1} for the isocitrate cleavage direction is significantly higher than the reported value of 5.2 s^{-1},[24] which can be attributed to the increased temperature used in the current studies. In the isocitrate synthesis direction, substrate inhibition by glyoxylate was observed at elevated concentrations, as was observed for ICL from *Phycomyces blakesleeanus*,[25] but in manner different from what was seen for this orthologue, no inhibition by succinate could be detected for *Mt*ICL (Figure S1 of the Supporting Information). Most ICLs, including those from *Pseudomonas indigofera*,[26] *Lupinus*,[27] and *Neurospora crassa*,[28] have been characterized as following an ordered sequential mechanism with glyoxylate (A) preceding succinate (B). The data with *Mt*ICL were therefore fit (eq 2) to a modified version of this ordered mechanism in which glyoxylate additionally binds the EA binary complex to yield a dead-end EA_2 complex. Confirming the ordered nature of the mechanism, we found succinate to be a noncompetitive inhibitor versus isocitrate (Figure S2 of the Supporting Information), while oxalate, a glyoxylate analogue, was found to be a competitive inhibitor versus isocitrate (Figure S3 of the Supporting Information) and glyoxylate (Figure S4 of the Supporting Information).

Table 1. Steady-State Kinetic Parameters for Isocitrate Cleavage and Synthesis by *Mt*ICL[a]

substrate[a]	k_{cat} (s^{-1})	K_m (μM)	K_{ia} (μM)[c]	K_i (mM)[c]
isocitrate	12.2 ± 0.6	45 ± 14[b]	N/A[d]	N/A[d]
succinate	8.5 ± 1.5	412 ± 6	N/A[d]	N/A[d]
glyoxylate		140 ± 4	30 ± 11	4.3 ± 0.2

[a]Parameters were obtained by fitting of initial velocities at pH 7.0 to eq 1 or 2. Errors are standard deviations. [b]K_m reflects only the reactive D enantiomer present in the racemate. [c]K_{ia} and K_i are the constants for dissociation of A (glyoxylate) from the EA complex and dead-end EA_2 complex, respectively. [d]Not applicable.

pH–Rate Profiles and Solvent Kinetic Isotope Effects. The pH dependence of the apparent k_{cat} and k_{cat}/K_b with the succinate concentration varied and the glyoxylate concentration fixed is shown in Figure 1 (blue points and curves). Data for k_{cat}/K_b were fit to eq 3, which describes a bell-shaped function with decreased rates in acidic and basic regions consistent with one and two ionizable groups, respectively. In the case of k_{cat}, the data conformed to a different bell-shaped function (eq 5), in which the rates decreased in the basic limb with a single titratable group, while the rates in the acidic region, also governed by a single ionizable group, decreased to a non-zero limit. Simpler models (i.e., with only one titratable group in the basic limb of the k_{cat}/K_b data and with a zero limiting acidic rate for the k_{cat} data) yielded similar R^2 values (0.87–0.95) but resulted in larger deviations at high and low pH values (Figure S5 and Table S1 of the Supporting Information).

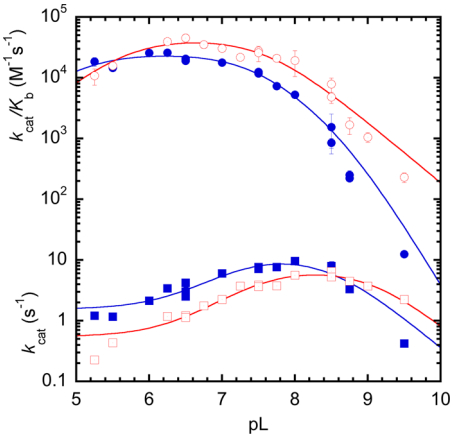

Figure 1. pL–rate profiles for *Mt*ICL-catalyzed synthesis of isocitrate at 500 μM glyoxylate and varying succinate concentrations. The apparent k_{cat}/K_b data in H_2O (filled blue circles) were fit to eq 3; apparent k_{cat}/K_b data in D_2O (empty red circles) were fit to eq 4, and apparent k_{cat} data in H_2O (filled blue squares) and D_2O (empty red squares) were fit to eq 5.

The pD dependence of the apparent rate constants was probed by repeating the measurements in D_2O (Figure 1, red points and curves). As expected, the pK values shifted to higher values, largely because of the lyonium ion's inverse fractionation factor ($\phi_{L_3O^+} = [D_3O^+]/[H_3O^+] = 0.69$ per H/D).[29] The poorly defined pK_3 observed in the apparent k_{cat}/K_b profile in H_2O could not be established in D_2O, possibly because of its expected increase and a lack of data at high pD, where K_b becomes large; a similar observation was made for the cysteine protease cathepsin C.[30]

A large inverse solvent kinetic isotope effect (KIE) on k_{cat}/K_b, $^{D_2O}(V/K_b)$, of 0.56 ± 0.07 was observed (Table 2). Control experiments containing 9% (w/v) glycerol,[31] which approximates the viscosity of D_2O, decreased k_{cat}/K_b and k_{cat} by 25%; because the effect of viscosity on k_{cat}/K_b is in opposition to that observed in D_2O, $^{D_2O}(V/K_b)$ cannot be attributed to differences in solvent viscosity. In contrast, a ^{D_2O}V of 1.7 ± 0.4 was observed, indicating that k_{cat} and k_{cat}/K_b include different isotope-sensitive steps.

pH Dependence of Inhibition Constants for Itaconate and 3-NP. Itaconate and 3-NP are succinate analogues (Scheme 1) that act as competitive inhibitors of ICL versus succinate (Figure S6 of the Supporting Information). Whereas itaconate shares a similar acidity with succinate, the C-3 protons of 3-NP have a pK of 9.1.[32] Because of this acidity, it has been suggested that the conjugate base, propionate-3-nitronate, serves as the true inhibitor by mimicking the aci form of the succinate trianion intermediate.[10] 3-NP has previously been characterized as a slow-binding inhibitor of ICL, displaying a time-dependent increase in the level of inhibition.[10]

dx.doi.org/10.1021/bi401432t | *Biochemistry* 2014, 53, 178–187

Table 2. Solvent Kinetic Isotope Effects and pL Dependence of Steady-State Kinetics for *Mt*ICL[a]

	solvent		
	H_2O	D_2O	kinetic isotope effect[b]
k_{cat} (s^{-1})	12 ± 2	7.3 ± 0.9	^{D_2O}V = 1.7 ± 0.4
γ	0.13 ± 0.04	0.07 ± 0.04	
pK values (k_{cat})	pK_1 = 7.2 ± 0.3	pK_1 = 7.49 ± 0.15	
	pK_2 = 8.5 ± 0.2	pK_2 = 9.10 ± 0.16	
k_{cat}/K_b (M^{-1} s^{-1})	(2.5 ± 0.2) × 10^4	(4.5 ± 0.5) × 10^4	$^{D_2O}(V/K_b)$ = 0.56 ± 0.07
pK values (k_{cat}/K_b)	pK_1 = 5.0 ± 0.2	pK_1 = 5.66 ± 0.18	
	pK_2 = 7.44 ± 0.17	pK_2 = 7.62 ± 0.14	
	pK_3 = 8.8 ± 1.4		

[a]Kinetic parameters obtained from fits of eq 3 (k_{cat}/K_b in H_2O), eq 4 (k_{cat}/K_b in D_2O), and eq 5 (k_{cat}) to the apparent rate constants. [b]Calculated from the pL-independent values of k_{cat}/K_b and k_{cat} obtained from c values in eqs 3−5.

This was confirmed for *Mt*ICL, and following overnight incubations of the inhibitor with the enzyme, the observed inhibition constant for the tight complex, K_i*, was found to be 44 ± 10 nM at pH 7.5, comparable to the value of ≤17 nM at pH 8 estimated by Schloss and Cleland with ICL from *P. indigofera*.[10] However, the C-3 protons of 3-NP exchange slowly with solvent over this extended period,[33] and because we desired to measure a solvent EIE on the inhibition constant (*vide infra*), we could not make use of K_i* for this purpose.[a] Therefore, we chose to measure the inhibition prior to formation of this final, tight complex by recording "initial velocities" only in the period approximately 1−3 min following initiation of the reaction.

We investigated the pH dependence of K_i for 3-NP and compared it with that for itaconate, which does not display slow-onset inhibition and lacks an acidic α-proton (Figure 2).

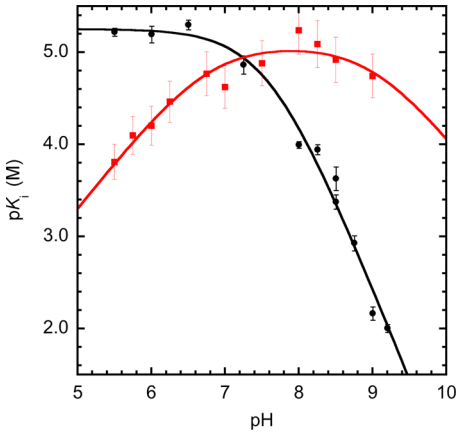

Figure 2. pH dependence of inhibition constants for the succinate analogues 3-NP (red squares) and itaconate (black circles). Curves represent fits to eqs 8 and 9, respectively.

The basic limb of itaconate's pH−pK_i profile is governed by two titratable groups with a pK_1 of 7.3 ± 0.4 and a pK_2 of 7.9 ± 0.4 (Table 3), both of which must be protonated for inhibitor binding. The pH−pK_i profile for 3-NP bears a striking contrast, exhibiting a bell-shaped profile characterized by a pK_1 of 6.77 ± 0.14 and a pK_2 of 9.0 ± 0.3.

Solvent Isotope Effects on Inhibition Constants. Weiss et al.[34] attempted to identify the catalytic base of enolase as a cysteine residue by measuring an EIE on K_i for an inhibitor possessing an acidic proton or deuteron. Enolase catalyzes deprotonation of D-tartronate semialdehyde phosphate (TSP), which is competitive with the substrate 2-phospho-D-glycerate, to generate an enolate, which serves as the true inhibitor (Scheme 2). According to this scheme and neglecting the enzyme that is bound with TSP in its conjugate acid form, we found $^{D}K_i$ is simply the ratio ϕ_{BL}/1.19, where ϕ_{BL} is the fractionation factor of the unknown enzymatic base and 1.19 is the fractionation factor assumed for TSP's exchangeable proton.[34] A $^{D}K_i$ of 0.41 ± 0.02 was observed, which led the authors to conclude that a sulfhydryl group was responsible for proton abstraction. This conclusion was later rescinded upon publication of the enzyme's crystallographic structure,[35] which showed there is no cysteine available to serve as the base; instead, low-barrier hydrogen bonds, which have low fractionation factors, were invoked.[36] In contrast, the crystal structure of *Mt*ICL bound with glyoxylate and 3-NP reveals that Cys191 is poised to serve as the catalytic base.

Despite the misinterpretation by Weiss et al., we have adopted their strategy for *Mt*ICL by measuring a solvent isotope effect on inhibition by 3-NP. We initially considered determining $^{D_2O}K_i$ as the ratio of the respective inhibition constants in H_2O and D_2O using the cuvette-based assays described above; however, this proved to be highly imprecise because of interference from the slow transition to the tight complex with 3-NP, as evidenced by the large error bars in the pH−pK_i profile (Figure 2). We therefore performed subsequent experiments with 3-NP in a stopped-flow apparatus. By extending the time window down to 0.06 s, we observed unexpectedly that 3-NP establishes the tightly inhibited complex over two time domains (i.e., a double-exponential decay function), in which the faster phase is nearly complete within the first 60 s, while the slower phase requires several minutes to hours. By limiting the acquisition to the first 60 s, we found the data conformed to a single-exponential process (Figure 3A), whose observed rate constant, k_{obs}, is dependent on 3-NP concentration and is noticeably larger in D_2O. The concentration dependence of k_{obs} was found to be linear, with an unchanged y-intercept but a larger slope for D_2O (Figure 3B).

DISCUSSION

pH−Rate and pH−pK_i Profiles. Assigning pK values in pH profiles to specific residues solely on the basis of their values is hazardous, especially when considering freely reversible reactions, in which microscopic reversibility may require reverse protonation for the opposing reaction direction.[37] Additional information (e.g., structural data) can assist in making more confident assignments. The pH dependence of

Table 3. Solvent Isotope Effects on Inhibition of *Mt*ICL by Itaconate and 3-Nitropropionate[a]

	itaconate		3-NP	
	H_2O	D_2O	H_2O	D_2O
pK values[b]	pK_1 = 7.3 ± 0.4	ND	pK_1 = 6.77 ± 0.14	ND
	pK_2 = 7.9 ± 0.4	ND	pK_2 = 9.0 ± 0.3	ND
k_{off} (s^{-1})[c]	N/A	N/A	(2.09 ± 0.12) × 10^{-3}	(2.03 ± 0.16) × 10^{-3}
$(k_{on})_{app}$ (M^{-1} s^{-1})[c]	N/A	N/A	305 ± 14	760 ± 40
$^{D_2O}(k_{on})_{app}$	N/A		0.40 ± 0.03	
K_i (μM)[d]	8.5 ± 0.9	8.2 ± 1.3	3.3 ± 0.2	1.25 ± 0.12
$^{D_2O}K_i$	1.0 ± 0.2		2.6 ± 0.3	

[a]ND, not determined; N/A, not applicable. [b]Determined from fits of eqs 9 and 8 to pK_i vs pH for itaconate and 3-NP, respectively. Errors are standard errors from nonlinear regression. [c]Calculated from fits of eq 11 to plots of k_{obs} vs [3-NP]. k_{obs} was obtained from fits of eq 10 to data acquired by stopped-flow spectroscopy. Errors are standard deviations from triplicate experiments. [d]Calculated from fits of eqs 6 and 7 to initial velocities for itaconate and from $k_{off}/[(k_{on})_{app}(1 + [B]/K_b)]$ for 3-NP. The value for 3-NP represents the apparent K_i that includes both isomeric enzyme forms.

Scheme 2. Mechanism for Isotope-Sensitive Inhibition of Enolase by D-Tartronate Semialdehyde Phosphate

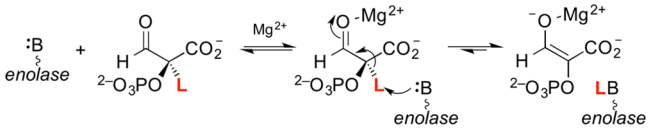

inhibition constants is most readily interpretable because it typically reflects only binding (except for 3-NP; *vide infra*), and therefore, the pK values represent those of the inhibitor or the enzyme form with which it binds. Binding by itaconate requires two residues (pK_1 of 7.3 and pK_2 of 7.9) to be protonated, suggesting that these may serve to stabilize one of the inhibitor's carboxylates through hydrogen bonding or ionic interactions. Although a crystal structure of the *Mt*ICL·glyoxylate·itaconate complex is not available, two ionizable groups, Arg228 and Glu285, form interactions with the nitro group[b] in the *Mt*ICL·glyoxylate·3-NP complex[7] and therefore could be involved in stabilizing the corresponding carboxylate in the itaconate complex. With an O−O separation of only 2.5 Å, Glu285 would be expected to have a particularly elevated pK, because it must be protonated to prevent electrostatic repulsion between the carboxylate groups; a similar observation has been made for the corresponding glutamate (Glu188) in 2-methylisocitrate lyase.[38]

Interestingly, the basic limb in itaconate's pH−pK_i profile resembles that in the pH−rate profile for the apparent k_{cat}/K_b of succinate (Figure 1), whose pK values of 7.44 and 8.8 are slightly higher. Therefore, it is likely that these reflect the same groups required for binding succinate's C-1 carboxylate (C-6 in isocitrate). Because of the short distance and matched intrinsic pK values, a hydrogen bond between this carboxylate and Glu285 would be expected to be particularly favorable (i.e., what has been described by others as a low-barrier hydrogen bond)[36,39] and would serve to acidify the proton at C-2 for the subsequent aldol reaction. The acid region of the k_{cat}/K_b profile features an ionizable group (pK_1 = 5.0) that is absent in the itaconate profile, suggesting that this group does not function in substrate binding. On the basis of the pK values of 4.2−4.5 observed for the nucleophilic thiol of several cysteine proteases,[30,40,41] we tentatively assign Cys191 to this pK. This residue is strictly conserved over all known ICLs and 2-methylisocitrate lyases[38] and is positioned 3.0 Å from C-3 of 3-NP (equivalent to C-2 of succinate);[7] therefore, it is reasonable to suggest that Cys191 serves as the general base (general acid in the isocitrate cleavage direction) for deprotonation of succinate during catalysis (Scheme 3). This value is significantly

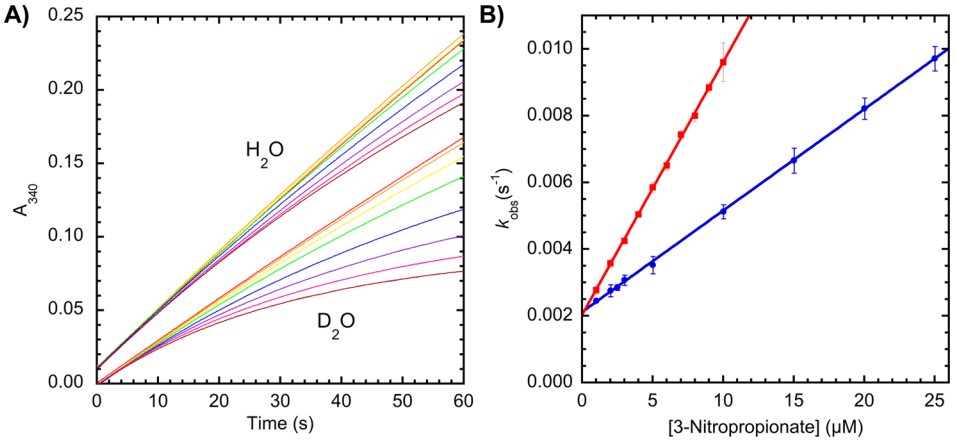

Figure 3. Slow-binding inhibition of *Mt*ICL by 3-NP in H_2O and D_2O. (A) Time dependence of isocitrate formation monitored by IDH-coupled formation of NADPH during the first 60 s of reaction in the presence of varying concentrations of 3-NP (0, 1.0, 2.5, 5.0, 10, 15, 20, and 25 μM from top to bottom, respectively) in H_2O or D_2O. The H_2O series has been vertically offset from the D_2O series for the sake of clarity. The data were fit by nonlinear regression to eq 10 (fits not shown). (B) Concentration dependence of observed slow-onset rate constants (k_{obs}) for 3-NP inhibition of *Mt*ICL in H_2O (circles) and D_2O (squares). Lines represent least-squares fits to eq 11.

dx.doi.org/10.1021/bi401432t | *Biochemistry* 2014, 53, 178−187

Scheme 3. Solvent-Sensitive Mechanism for *Mt*ICL-Catalyzed Isocitrate Synthesis[a]

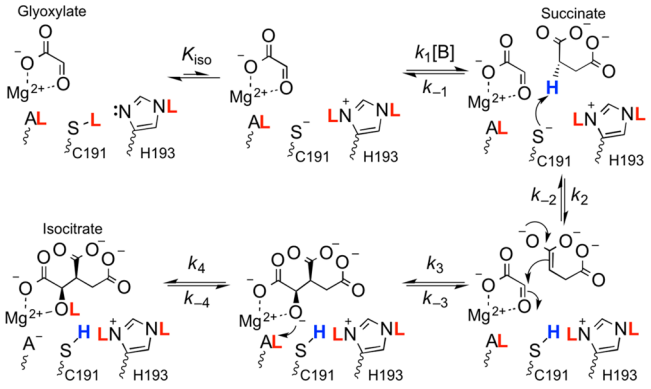

[a]Binding of glyoxylate, the first step in the ordered mechanism, does not affect k_{cat} or k_{cat}/K_b and has been omitted for the sake of clarity. L represents H in H_2O or D in D_2O.

lower than the pK of 7.4 reported for alkylation of Cys195 of *E. coli* ICL by 3-bromopyruvate;[42] however, it is important to note that alkylation, performed on unliganded enzyme, and catalysis, performed with enzyme saturated with Mg^{2+}-bound glyoxylate, involve different reactions with different microenvironments.

The pH dependence of inhibition by 3-NP (Figure 2) contrasts that by itaconate. The basic limb of the former lacks the two pK values present in the latter, consistent with the functional group change in the inhibitors (i.e., from an anionic carboxylate to a neutral nitro group), assuming that the residues associated with these pK values are responsible for charge stabilization (*vide supra*). Instead, a pK_2 of 9.0 was observed, most likely due to the C-3 proton of 3-NP (pK = 9.1). Because the level of inhibition decreases as this proton is removed, it is evident that if the nitronate form is the true inhibitor, it does not bind to the free enzyme and therefore is generated while 3-NP is bound to the enzyme. This conclusion is at odds with the work of Schloss and Cleland,[10] who assumed that a net charge of −2 (present in succinate, itaconate, and propionate-3-nitronate) was obligatory for binding. Absent from the itaconate profile, a group with a pK_1 of 6.77 must be unprotonated for maximal inhibition by 3-NP. Because of its proximity and proposed role as a general base in deprotonation of succinate, we assign this pK to Cys191 and suggest that it serves an analogous role in deprotonating the inhibitor (*vide infra*). If this assignment is correct, it indicates that the acidity of Cys191 is highly sensitive to the bound state of the enzyme, as was mentioned earlier, shifting from a pK of 5 when only glyoxylate is bound to a value of ∼7 with 3-NP bound. Consistent with this, a similar pK of 7.2 was observed when the enzyme was bound with succinate [k_{cat}−pH profile (Figure 1)]. The fact that *Mt*ICL follows an ordered sequential kinetic mechanism that permits binding of only succinate after glyoxylate is also indicative of active site changes related to the enzyme's bound state.

The group with a pK_2 of 8.5 in the pH−rate profile for k_{cat} must be protonated for maximal activity. The identity of this residue is unknown but could be the general acid required for protonation of the alkoxide to form isocitrate ("AL" in Scheme 3). Possible candidates include Arg228, Tyr89, and His180, which are each within 4 Å of glyoxylate's aldehyde oxygen[7] and are also present in other ICLs.[8]

Solvent Kinetic Isotope Effects. The chemical mechanism depicted in Scheme 3 requires at least two solvent-derived proton transfers, one from Cys191 (possibly to N_δ of His193) and the other to the alkoxide following C−C bond formation. Although either process could be partially rate-limiting, as was suggested for the isocitrate cleavage reaction,[24] the inverse nature of the observed $^{D_2O}(V/K_b)$ indicates that this is largely the result of an equilibrium isotope effect (EIE). Inverse solvent KIEs have also been reported for cysteine proteases, including the acylation half-reaction of papain[43] and k_{cat}/K_m for cathepsin C.[30] In the latter case, Meek and colleagues accounted for the inverse KIE by invoking a prebinding isomerization (or "tautomerization") of the thiol−imidazole pair of the active site Cys−His dyad to form the reactive thiolate−imidazolium pair.[30] By direct analogy, we propose that Cys191 is prepared for serving as the general base only after its proton had been transferred to His193 in a prebinding equilibrium governed by K_{iso} (Scheme 3). This process is assumed to be in rapid equilibrium during catalysis and largely unfavorable in this direction (i.e., $K_{iso} \ll 1$); however, because of the inverse fractionation factor on the sulfhydryl group, this is favored in D_2O. Assuming typical fractionation factors for sulfhydryl (R-SL), imidazole (R-NL), and imidazolium (R-NL$^+$) of 0.4−0.6, 1.12, and 1.08,[44] respectively, a theoretical solvent EIE on isomerization of 0.38−0.58 can be calculated from eq 12.

$$^{D_2O}K_{iso} = \frac{[\text{R-SD}][\text{R-ND}][\text{R-NH}^+]^2}{[\text{R-SH}][\text{R-NH}][\text{R-ND}^+]^2} = \frac{\phi_{SL}\phi_{NL}}{\phi_{NL^+}^2} \quad (12)$$

Thus, fractionation factors can account for the entire observed $^{D_2O}(V/K_b)$.

According to this mechanism, when the enzyme is saturated with succinate, the forms of the enzyme that gave rise to $^{D_2O}K_{iso}$ no longer exist. The normal KIE on k_{cat} therefore reflects the loss of this inverse contribution and largely reflects a kinetic effect due to proton transfer, presumably during formation of isocitrate's alcohol (Scheme 3, step 4). The value of 1.7 is small for a primary KIE, suggesting that this step is only partially rate limiting for k_{cat}. The fact that this normal KIE does not also contribute to $^{D_2O}(V/K_b)$ indicates that (1) the forward commitment (i.e., the tendency for the substrate to undergo a transition through the isotope-sensitive step vs dissociation) for k_{cat}/K_b is much greater than that for k_{cat}, which could be the case if succinate is "sticky", or (2) there is an irreversible step prior to step 4. This situation is remarkably similar to that observed for malate synthase from *M. tuberculosis*. Malate synthase, which immediately follows ICL in the glyoxylate cycle, catalyzes a similar aldol reaction between glyoxylate and acetyl-CoA. Quartararo and Blanchard[45] reported a $^{D_2O}(V/K)$ of 0.6 and a ^{D_2O}V of 1.5 for [*methyl*-$^2H_3$]acetyl-CoA and proposed that the first irreversible step is C−C bond formation to generate an alkoxide; protonation of the alkoxide with a solvent-derived proton/deuteron gives rise to the normal KIE observed only in ^{D_2O}V. By analogy, we propose that C−C bond formation (i.e., step 4) is the first effectively irreversible step for *Mt*ICL in the synthesis direction; this step would be expected to be highly favorable considering the relative stabilities of the succinate trianion (conjugate acid pK of >33)[46] and isocitrate alkoxide (conjugate acid pK of ∼18). Additional experiments, such as substrate ^2H, ^{13}C, and mixed isotope KIE measurements, are necessary to resolve these possibilities.

Slow-Onset Inhibition and Solvent Isotope Effect on K_i for 3-NP. Two common mechanisms that account for slow-

dx.doi.org/10.1021/bi401432t | *Biochemistry* 2014, 53, 178−187

Scheme 4. Solvent-Sensitive Mechanism for *Mt*ICL Inhibition by 3-NP[a]

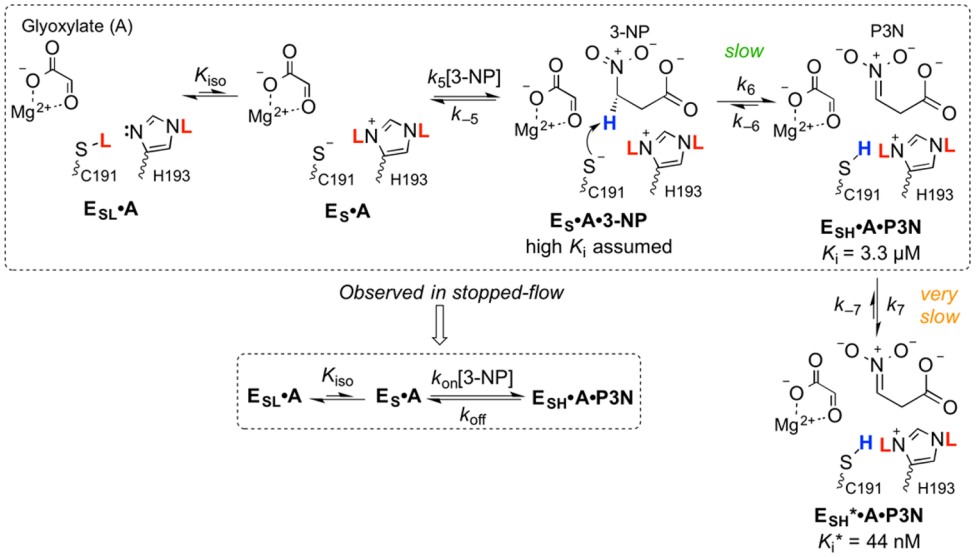

[a]The dashed box indicates the portion of the mechanism that can be observed in the stopped-flow experiments. Abbreviations: P3N, propionate-3-nitronate; E_{SL}/E_{SH}, enzyme with Cys191 in thiol form; E_S, enzyme with Cys191 in thiolate form; L, H in H_2O or D in D_2O.

onset inhibition are (1) slow, one-step binding and (2) two-step binding in which a slow second step follows formation of the initial complex.[22] Schloss and Cleland[10] used the latter case to account for the slow-binding inhibition of *P. indigofera* ICL by 3-NP, which they proposed was bound only in its nitronate form following nonenzymatic ionization. By using a stopped-flow instrument, we were able to identify an additional time-dependent increase in the level of inhibition on a much shorter time scale (0−60 s) with *Mt*ICL, and therefore, the mechanism for inhibition requires at least one additional step. We hypothesize that binding of 3-NP proceeds over three steps in which (1) a weak encounter complex (E_S·A·3-NP) is formed, followed by (2) the slow deprotonation by Cys191 to form the nitronate, which is bound with micromolar affinity (E_{SH}·A·P3N), and (3) a very slow conformational change that results in the final complex (E_{SH}*·A·P3N) with nanomolar affinity (Scheme 4). Like catalysis with succinate, this mechanism requires Cys191 to be in the thiolate form, so the same prebinding isomerization can be expected.

The one-step and two-step mechanisms for slow-binding inhibition are often distinguished by their linear and hyperbolic concentration dependence, respectively. Because we observed a linear dependence on k_{obs} during the 0−60 s time domain, this would suggest that 3-NP binds to *Mt*ICL in a one-step process. However, such a mechanism would not be expected to require the thiolate−imidazolium form of the enzyme and therefore would not be expected to yield a solvent isotope effect on k_{obs}. As described by Morrison and Walsh,[22] under the condition that $[3\text{-NP}] \ll K_{-5}(1 + [B]/K_b)$ (K_{-5} is the K_i for the E_S·A·3-NP complex in Scheme 4, top), the steady-state concentration of the E_S·A·3-NP is insignificant, and the E_{SL}·A complex is observed to form the E_{SH}·A·P3N complex directly (Scheme 4, bottom). This situation would lead to a linear concentration dependence of k_{obs}, in which the *y*-intercept is the net rate constant for dissociation, k_{off}, and the slope is the apparent rate constant for association, $(k_{on})_{app}$ (eq 11). k_{off} was identical in H_2O and D_2O (Table 3), as would be expected if no solvent-derived proton is involved in dissociation (Scheme 4). In contrast, $(k_{on})_{app}$ was larger in D_2O. Because the enzyme form that binds and deprotonates 3-NP is the minor component and also binds succinate competitively, $(k_{on})_{app}$ is smaller than k_{on}, the true net rate constant for binding and ionization of 3-NP, according to eq 13.

$$(k_{on})_{app} = \left(\frac{K_{iso}}{K_{iso} + 1}\right)\left(\frac{1}{1 + \frac{[B]}{K_b}}\right)k_{on} \quad (13)$$

The observed solvent isotope effect on $(k_{on})_{app}$ is given by eq 14.

$${}^{D_2O}(k_{on})_{app} = \left(\frac{{}^{D_2O}K_{iso} + K_{iso}}{1 + K_{iso}}\right)\left[\frac{1 + \frac{[B]}{(K_b)_{D_2O}}}{1 + \frac{[B]}{(K_b)_{H_2O}}}\right]{}^{D_2O}k_{on} \quad (14)$$

When isomerization is unfavorable (i.e., $K_{iso} \ll 1$, ${}^{D_2O}K_{iso}$), eq 14 simplifies to eq 15, which can be rearranged for ${}^{D_2O}K_{iso}$ (eq 16).

$${}^{D_2O}(k_{on})_{app} = {}^{D_2O}K_{iso}\left[\frac{1 + \frac{[B]}{(K_b)_{D_2O}}}{1 + \frac{[B]}{(K_b)_{H_2O}}}\right]{}^{D_2O}k_{on} \quad (15)$$

$${}^{D_2O}K_{iso} = \left[\frac{{}^{D_2O}(k_{on})_{app}}{{}^{D_2O}k_{on}}\right]\left[\frac{1 + \frac{[B]}{(K_b)_{H_2O}}}{1 + \frac{[B]}{(K_b)_{D_2O}}}\right] \quad (16)$$

Taking ${}^{D_2O}k_{on}$ to be unity, as required for the proposed mechanism, and substituting the values of 500 μM for [B], 457 ± 9 μM for $(K_b)_{H_2O}$, and 438 ± 6 μM for $(K_b)_{D_2O}$ yield a ${}^{D_2O}K_{iso}$ of 0.39 ± 0.03, which also falls within the range of 0.38−0.58 estimated from fractionation factors (eq 12). The similarity in magnitudes of the inverse solvent isotope effects measured on k_{cat}/K_m for succinate and $(k_{on})_{app}$ for 3-NP is therefore consistent with a common mechanism involving an unfavorable isomerization of the Cys191−His193 pair to the

dx.doi.org/10.1021/bi401432t | *Biochemistry* 2014, 53, 178−187

thiolate−imidazolium form prior to ligand binding and proton transfer.

As a test of our hypothesis, we measured K_i values of 8.5 ± 0.9 and 8.2 ± 1.3 μM for itaconate in H_2O and D_2O, respectively, yielding a $^{D_2O}K_i$ of 1.0 ± 0.2 (Table 3). This result serves as an important control, indicating that the solvent isotope effect is unique to 3-NP and that itaconate is capable of binding effectively to the abundant thiol−imidazole enzyme form. This outcome reinforces the conclusion from our pH dependence studies that ICL does not directly bind the nitronate form of the inhibitor and that 3-NP is a noncovalent mechanism-based inhibitor.[47] Interestingly, when solutions of 3-NP in D_2O were allowed to incubate at room temperature for >3 h prior to the measurement of slow-binding inhibition, the slope of the k_{obs} versus [3-NP] plots decreased to eventually become equivalent to that measured in H_2O (Figure S7 of the Supporting Information). This is explained by the slow exchange of deuterium into C-3 of 3-NP, forcing Cys191 to accept a deuteron instead of a proton during formation of propionate-3-nitronate. This introduces fractionation factors on K_6 that exactly oppose those in K_{iso}, resulting in a $^{D_2O}K_i$ of only 1.04.

In summary, this work shows evidence of Cys191 acting as the catalytic base necessary for synthesis of isocitrate from glyoxylate and succinate. Inverse solvent isotope effects were seen on both k_{cat}/K_m for succinate and the apparent rate of association of the succinate analogue 3-NP. These results are consistent with the unique inverse fractionation factors of thiols and indicate that Cys191 serves not only to ionize succinate for catalytic turnover but also in the mechanism-based inhibition by 3-NP. The inverse isotope effects are explained by a pre-equilibrium isomerization of the Cys−His pair to the unfavorable but reactive thiolate−imidazolium form, which is enriched in D_2O. The switch from an inverse KIE for $^{D_2O}(V/K_b)$ to a normal KIE for ^{D_2O}V indicates either that binding of succinate is highly committed or that the two solvent isotope-sensitive steps are separated by an effectively irreversible step, possibly C−C bond formation. These mechanistic details may assist efforts to design potent inhibitors of isocitrate lyase for the treatment of persistent tuberculosis.

■ ASSOCIATED CONTENT

Supporting Information

Lineweaver−Burk plots and globally fit kinetic parameters for *Mt*ICL-catalyzed isocitrate cleavage and synthesis in the presence and absence of inhibitors, an alternative fitting to pL−rate profiles, and the effect of solvent exchange into 3-NP on slow-binding inhibition. This material is available free of charge via the Internet at http://pubs.acs.org.

■ AUTHOR INFORMATION

Corresponding Author

*E-mail: amurkin@buffalo.edu. Telephone: (716) 645-4249. Fax: (716) 645-6963.

Funding

This work was supported by funds from the University at Buffalo and National Science Foundation CAREER Award CHE1255136.

Notes

The authors declare no competing financial interest.

■ ACKNOWLEDGMENTS

This paper is dedicated to the life of W. W. (Mo) Cleland.

■ ABBREVIATIONS

EIE, equilibrium isotope effect; ICL, isocitrate lyase; IDH, isocitrate dehydrogenase; IPTG, isopropyl β-D-1-thiogalactopyranoside; KIE, kinetic isotope effect; LDH, lactate dehydrogenase; *Mt*ICL, *M. tuberculosis* isocitrate lyase; 3-NP, 3-nitropropionate; P3N, propionate-3-nitronate; TSP, D-tartronate semialdehyde phosphate.

■ ADDITIONAL NOTES

[a] A $^{D_2O}K_i$* of 1.1 ± 0.3 was obtained when measuring K_i* after overnight incubations of 3-NP with *Mt*ICL in H_2O and D_2O. This isotope effect near unity is consistent with the incorporation of deuterium into C-3 of 3-NP such that Cys191 is forced to replace its solvent-derived deuteron with a deuteron from the inhibitor instead of a proton.

[b] Because of their isosteric nature, it is not possible to assign unambiguously the carboxylate and nitro groups of 3-NP in the crystal structure (Protein Data Bank entry 1F8I) of the *Mt*ICL·glyoxylate·3-NP complex. Our assignment is based on the assumption that the methylene group that is best positioned for reaction with glyoxylate is the more acidic C-3 of 3-NP (equivalent to C-2 of succinate). However, the discussion is not affected if the assignments are reversed.

■ REFERENCES

(1) McKinney, J. D., Honer zu Bentrup, K., Munoz-Elias, E. J., Miczak, A., Chen, B., Chan, W. T., Swenson, D., Sacchettini, J. C., Jacobs, W. R., Jr., and Russell, D. G. (2000) Persistence of *Mycobacterium tuberculosis* in macrophages and mice requires the glyoxylate shunt enzyme isocitrate lyase. *Nature 406*, 735−738.

(2) Britton, K., Langridge, S., Baker, P. J., Weeradechapon, K., Sedelnikova, S. E., De Lucas, J. R., Rice, D. W., and Turner, G. (2000) The crystal structure and active site location of isocitrate lyase from the fungus *Aspergillus nidulans*. *Structure 8*, 349−362.

(3) Wayne, L. G., and Lin, K. Y. (1982) Glyoxylate metabolism and adaptation of *Mycobacterium tuberculosis* to survival under anaerobic conditions. *Infect. Immun. 37*, 1042−1049.

(4) Munoz-Elias, E. J., and McKinney, J. D. (2005) *Mycobacterium tuberculosis* isocitrate lyases 1 and 2 are jointly required for in vivo growth and virulence. *Nat. Med. 11*, 638−644.

(5) Sprecher, M., Berger, R., and Sprinson, D. B. (1964) Stereochemical course of the isocitrate lyase reaction. *J. Biol. Chem. 239*, 4268−4271.

(6) Sprecher, M., Berger, R., and Sprinson, D. B. (1964) Stereochemical Course of the Isocitrate Lyase Reaction. *J. Biol. Chem. 239*, 4268−4271.

(7) Sharma, V., Sharma, S., zu Bentrup, K. H., McKinney, J. D., Russell, D. G., Jacobs, W. R., and Sacchettini, J. C. (2000) Structure of isocitrate lyase, a persistence factor of *Mycobacterium tuberculosis*. *Nat. Struct. Mol. Biol. 7*, 663−668.

(8) Britton, K. L., Abeysinghe, I. S., Baker, P. J., Barynin, V., Diehl, P., Langridge, S. J., McFadden, B. A., Sedelnikova, S. E., Stillman, T. J., Weeradechapon, K., and Rice, D. W. (2001) The structure and domain organization of *Escherichia coli* isocitrate lyase. *Acta Crystallogr. D57*, 1209−1218.

(9) Rehman, A., and McFadden, B. A. (1997) Cysteine 195 has a critical functional role in catalysis by isocitrate lyase from *Escherichia coli*. *Curr. Microbiol. 35*, 267−269.

(10) Schloss, J. V., and Cleland, W. W. (1982) Inhibition of isocitrate lyase by 3-nitropropionate, a reaction-intermediate analog. *Biochemistry 21*, 4420−4427.

(11) Cole, S. T., Brosch, R., Parkhill, J., Garnier, T., Churcher, C., Harris, D., Gordon, S. V., Eiglmeier, K., Gas, S., Barry, C. E., III, et al. (1998) Deciphering the biology of *Mycobacterium tuberculosis* from the complete genome sequence. *Nature 393*, 537−544.
(12) Dixon, G. H., and Kornberg, H. L. (1959) Assay methods for key enzymes in the glyoxylate cycle. *Proc. Biochem. Soc.*, 3P.
(13) Bradford, M. M. (1976) A rapid and sensitive method for the quantitation of microgram quantities of protein utilizing the principle of protein-dye binding. *Anal. Biochem. 72*, 248−254.
(14) Kitagawa, M., Ara, T., Arifuzzaman, M., Ioka-Nakamichi, T., Inamoto, E., Toyonaga, H., and Mori, H. (2005) Complete set of ORF clones of *Escherichia coli* ASKA library (A complete set of *E. coli* K-12 ORF archive): Unique resources for biological research. *DNA Res. 12*, 291−299.
(15) Honer Zu Bentrup, K., Miczak, A., Swenson, D. L., and Russell, D. G. (1999) Characterization of activity and expression of isocitrate lyase in *Mycobacterium avium* and *Mycobacterium tuberculosis*. *J. Bacteriol. 181*, 7161−7167.
(16) Warren, W. A. (1970) Catalysis of both oxidation and reduction of glyoxylate by pig heart lactate dehydrogenase isozyme 1. *J. Biol. Chem. 245*, 1675−1681.
(17) Billo, E. J. (1997) *Excel for chemists: A comprehensive guide*, Wiley-VCH, New York.
(18) Segel, I. H. (1975) *Enzyme kinetics: Behavior and analysis of rapid equilibrium and steady state enzyme systems*, p 823, Wiley, New York.
(19) Salomaa, P., Schaleger, L. L., and Long, F. A. (1964) Solvent Deuterium Isotope Effects on Acid-Base Equilibria. *J. Am. Chem. Soc. 86*, 1−7.
(20) Cook, P. F., and Cleland, W. W. (2007) *Enzyme Kinetics and Mechanism*, pp 325−358, Taylor & Francis, New York.
(21) Koudelka, G. B., Hansen, F. B., and Ettinger, M. J. (1985) Solvent isotope effects and the pH dependence of laccase activity under steady-state conditions. *J. Biol. Chem. 260*, 15561−15565.
(22) Morrison, J. F., and Walsh, C. T. (1988) The behavior and significance of slow-binding enzyme-inhibitors. *Adv. Enzymol. Relat. Areas Mol. Biol. 61*, 201−301.
(23) Johnson, K. A. (1992) Transient-State Kinetic Analysis of Enzyme Reaction Pathways. In *The Enzymes* (David, S. S., Ed.) pp 1−61, Academic Press, San Diego.
(24) Quartararo, C. E., Hadi, T., Cahill, S. M., and Blanchard, J. S. (2013) Solvent isotope-induced equilibrium perturbation for isocitrate lyase. *Biochemistry 52*, 9286−9293.
(25) Rua, J., de Arriaga, D., Busto, F., and Soler, J. (1990) Isocitrate lyase from *Phycomyces blakesleeanus*. The role of Mg^{2+} ions, kinetics and evidence for two classes of modifiable thiol groups. *Biochem. J. 272*, 359−367.
(26) Williams, J. O., Roche, T. E., and McFadden, B. A. (1971) Mechanism of action of isocitrate lyase from *Pseudomonas indigofera*. *Biochemistry 10*, 1384−1390.
(27) Vincenzini, M. T., Vanni, P., Giachetti, E., Hanozet, G. M., and Pinzauti, G. (1986) Steady-state kinetic analysis of isocitrate lyase from *Lupinus* seeds: Considerations on a possible catalytic mechanism of isocitrate lyase from plants. *J. Biochem. 99*, 375−383.
(28) Johanson, R. A., Hill, J. M., and McFadden, B. A. (1974) Isocitrate lyase from *Neurospora crassa*. I. Purification, kinetic mechanism, and interaction with inhibitors. *Biochim. Biophys. Acta 364*, 327−340.
(29) Schowen, K. B., and Schowen, R. L. (1982) Solvent isotope effects on enzyme-systems. *Methods Enzymol. 87*, 551−606.
(30) Schneck, J. L., Villa, J. P., McDevitt, P., McQueney, M. S., Thrall, S. H., and Meek, T. D. (2008) Chemical mechanism of a cysteine protease, cathepsin C, as revealed by integration of both steady-state and pre-steady-state solvent kinetic isotope effects. *Biochemistry 47*, 8697−8710.
(31) Karsten, W. E., Lai, C.-J., and Cook, P. F. (1995) Inverse solvent isotope effects in the NAD-malic enzyme reaction are the result of the viscosity difference between D_2O and H_2O: Implications for solvent isotope effect studies. *J. Am. Chem. Soc. 117*, 5914−5918.
(32) Bush, M. T., Touster, O., and Brockman, J. E. (1951) The production of β-nitropropionic acid by a strain of *Aspergillus flavus*. *J. Biol. Chem. 188*, 685−693.
(33) Bernasconi, C. F. (1987) Intrinsic Barriers of Reactions and the Principle of Nonperfect Synchronization. *Acc. Chem. Res. 20*, 301−308.
(34) Weiss, P. M., Boerner, R. J., and Cleland, W. W. (1987) The catalytic base of enolase is a sulfhydryl-group. *J. Am. Chem. Soc. 109*, 7201−7202.
(35) Lebioda, L., and Stec, B. (1991) Mechanism of enolase: The crystal structure of enolase−Mg^{2+}−2-phosphoglycerate/phosphoenol-pyruvate complex at 2.2-Å resolution. *Biochemistry 30*, 2817−2822.
(36) Cleland, W. W. (1992) Low-barrier hydrogen-bonds and low fractionation factor bases in enzymatic-reactions. *Biochemistry 31*, 317−319.
(37) Frey, P. A., and Hegeman, A. D. (2006) *Enzymatic Reaction Mechanisms*, p 115, Oxford University Press, Oxford, U.K.
(38) Liu, S., Lu, Z., Han, Y., Melamud, E., Dunaway-Mariano, D., and Herzberg, O. (2005) Crystal structures of 2-methylisocitrate lyase in complex with product and with isocitrate inhibitor provide insight into lyase substrate specificity, catalysis and evolution. *Biochemistry 44*, 2949−2962.
(39) Cleland, W. W., and Kreevoy, M. M. (1994) Low-barrier hydrogen bonds and enzymic catalysis. *Science 264*, 1887−1890.
(40) Ascenzi, P., Aducci, P., Torroni, A., Amiconi, G., Ballio, A., Menegatti, E., and Guarneri, M. (1987) The pH dependence of pre-steady-state and steady-state kinetics for the papain-catalyzed hydrolysis of N-α-carbobenzoxyglycine p-nitrophenyl ester. *Biochim. Biophys. Acta 912*, 203−210.
(41) Dolenc, I., Turk, B., Pungercic, G., Ritonja, A., and Turk, V. (1995) Oligomeric structure and substrate induced inhibition of human cathepsin C. *J. Biol. Chem. 270*, 21626−21631.
(42) Ko, Y. H., and McFadden, B. A. (1990) Alkylation of isocitrate lyase from *Escherichia coli* by 3-bromopyruvate. *Arch. Biochem. Biophys. 278*, 373−380.
(43) Polgar, L. (1979) Deuterium isotope effects on papain acylation. Evidence for lack of general base catalysis and for enzyme−leaving-group interaction. *Eur. J. Biochem. 98*, 369−374.
(44) Quinn, D. M. (2006) Theory and practice of solvent isotope effects. In *Isotope Effects in Chemistry and Biology* (Kohen, A. L., and Limbach, H.-H., Eds.) pp 995−1018, CRC Press LLC, Boca Raton, FL.
(45) Quartararo, C. E., and Blanchard, J. S. (2011) Kinetic and chemical mechanism of malate synthase from *Mycobacterium tuberculosis*. *Biochemistry 50*, 6879−6887.
(46) Richard, J. P., Williams, G., O'Donoghue, A. C., and Amyes, T. L. (2002) Formation and stability of enolates of acetamide and acetate anion: An Eigen plot for proton transfer at α-carbonyl carbon. *J. Am. Chem. Soc. 124*, 2957−2968.
(47) Silverman, R. B., and Hoffman, S. J. (1984) The organic chemistry of mechanism-based enzyme inhibition: A chemical approach to drug design. *Med. Res. Rev. 4*, 415−447.